THE JOURNAL OF PHYSICAL CHEMISTRY B

Article

Effect of Hofmeister Series Anions on the Thermotropic Phase Behavior of Bioactive *O*-Acylcholines

Pradip Kumar Tarafdar, S. Thirupathi Reddy, and Musti Joginadha Swamy

J. Phys. Chem. B, **Just Accepted Manuscript** • DOI: 10.1021/jp403964k • Publication Date (Web): 02 Aug 2013

Effect of Hofmeister Series Anions on the Thermotropic Phase Behavior of Bioactive *O*-Acylcholines

Pradip K. Tarafdar, S. Thirupathi Reddy and Musti J. Swamy*

School of Chemistry, University of Hyderabad, Hyderabad - 500 046, India

Running Title: Phase behavior of *O*-acylcholines

---

*Corresponding author:

Prof. Musti J. Swamy

School of Chemistry

University of Hyderabad

Hyderabad - 500 046, India

Tel: +91-40-2313-4807

Fax: +91-40-2301-2460

E-mail: mjssc@uohyd.ernet.in, mjswamy1@gmail.com

ABSTRACT

O-Acylcholines (OACs), which are true cationic lipids due to the quaternary ammonium functionality in the head group, exhibit interesting biological activities and medicinal properties. In the present study, a homologous series of OACs with even chainlengths (*n* = 12-20) have been synthesized and their thermotropic and chaotropic phase transitions have been characterized. The role of various anions (Cl^-, Br^-, I^-, NO_3^-, SO_4^{2-}, ClO_3^-, ClO_4^-) on the phase behavior of *O*-stearoylcholine was investigated by calorimetric, spectroscopic and turbidimetric approaches. The results obtained revealed that in aqueous dispersion *O*-stearoylcholine undergoes a cooperative phase transition from a gel phase to a micellar structure and that the transition temperature increases when the counterions are changed in the Hofmeister series. Single-crystal X-ray diffraction studies showed that *O*-stearoylcholine iodide forms an interdigitated bilayer structure, with the polymethylene chain adopting an all-trans conformation. The Hofmeister effect and phase behavior were explained using the concepts of *matching water affinities*, *water penetration into the bilayer* and *electrostatic repulsion*. It was also observed that one counterion per molecule is sufficient to strongly modulate the phase properties of the lipid/surfactant.

Keywords: Differential scanning calorimetry; X-ray diffraction; electron spin resonance; Krafft temperature; surfactant

INTRODUCTION

An important characteristic of surfactants is their tendency to precipitate from aqueous solutions, which can inhibit their activity and hence their use in many applications. The precipitation of surfactants occurs below a characteristic temperature – known as Krafft temperature – where surfactants are largely separated from the bulk medium and their surface activities are significantly decreased.[1,2] Above Krafft temperature the solubility of surfactants increases dramatically in aqueous systems, and is interpreted as the melting temperature of a hydrated solid surfactant.[1,3] Since below Krafft temperature surfactants separate out from the system, to keep the surfactants in their active form, it is desirable to lower the Krafft temperature. It has been shown that Krafft temperature is influenced by the ions present in solution.[1,4] The influence of ions on the phase behavior of lipids/surfactants has been studied extensively.[5-19] In alkyltrimethylammonium surfactants the ability of counterions to induce the sphere-to-rod transition follows the Hofmeister sequence[20,21] and in dodecyltrimethylammonium micelles, the aggregation numbers have been shown to increase along the Hofmeister sequence of the counterions.[22,23] Recently, the influence of acyl chain length on the phase behavior of surfactants were investigated.[24-26] However, the influence of Hofmeister series of ions on the modulation of Krafft temperature in a homologous series and associated thermodynamics have not been investigated in detail. It is known that chaotropic ions in the Hofmeister series make insoluble ion pairs with cationic surfactants,[21,27] whereas kosmotropic ions likely remain hydrated depending on the surfactant headgroup.[28] Mechanistic interpretation of how ions modulate the Krafft temperature from a standard model, for example, gel-micelle transition model is important to understand the role of ions on the phase properties of ionic lipids/surfactants. In view of this, in the present study tried

to address the following questions. 1) How do ions modulate the Krafft temperature of a homologous series of surfactants and what are the thermodynamics associated with it? 2) How many ions per each surfactant molecule are required for this modulation? 3) What is the 3-dimentional structure of solid precipitate appearing below Krafft temperature? 4) Is the modulation of the activity of surfactants/lipids by chaotropic ions different from the way they affect the activity of nucleic acids and proteins? To address these questions we chose a homologous series of *O*-acylcholines, which are bioactive surfactants about which very little is known with regard to their supramolecular structure and interactions with ions.

O-Acylcholines (OACs) are fatty acid esters of choline, which are true cationic lipids due to the quaternary ammonium functionality in the head group. OACs with different fatty acyl chains exhibit hemolytic activity, which is comparable to that of acylcarnitines and lysolecithins.[29,30] *O*-Palmitoylcholine, isolated from the skin secretions of smooth trunk fish (*Lactophrus triqueter* Linn.), exhibits toxicity against mosquitofish at low (ppm) concentration.[31] Several long-chain acylcholines were reported to inhibit wheat embryo Ca^{2+}-dependent protein kinase.[32] Beside these biological properties, OACs attract interest due to their medicinal properties. For example, OACs with various fatty acyl chains modulate blood pressure,[33] act as skin penetration enhancers for the transdermal delivery of drugs such as acyclovir, 17β-estradiol, hydrocortisone etc.,[34] and exhibit antimicrobial activity against a wide range of microorganisms.[35] As the OACs are enzymatically hydrolyzed to eco-friendly components, they can potentially replace the more toxic, stable quaternary ammonium compounds.[35] Although, as indicated above, the biological and pharmacological properties of OACs have been investigated in considerable detail, very little is known regarding their supramolecular structure, thermotropic phase transitions and interaction with anions. In view

of this lacuna, in the present study we have synthesized a homologous series of *O*-acylcholine iodides (OACs) with even chains and characterized their thermotropic phase transitions using DSC. The phase behavior of one of the OACs, namely *O*-stearoylcholine iodide (OSC) has been examined in the presence of sodium salts of various anions belonging to the Hofmeister series, viz., NaCl, Na_2SO_4, $NaNO_3$, NaBr, $NaClO_3$, $NaClO_4$ and NaI using differential scanning calorimetry (DSC), electron spin resonance (ESR) spectroscopy, turbidimetry and fluorescence spectroscopy. The results obtained indicate that counterions modulate the phase behavior of OSC and changing the counterion can induce a transition from a gel phase to a liquid crystalline phase, which we refer to as *chaotropic phase transition* and predict that other OACs would behave similarly. Finally, the 3-dimentional structure and packing of OSC was determined by single crystal X-ray diffraction, which revealed that the acyl chains are packed in an interdigitated manner.

MATERIALS AND METHODS

Materials. Fatty acids, stearic acid spin labeled on the 5th C-atom (5-SASL), *N, N'*-dicyclohexylcarbodiimide (DCC), 4-dimethylaminopyridine (DMAP), methyl iodide, sodium chloride, sodium bromide, sodium iodide, sodium nitrate, sodium sulfate, sodium chlorate and sodium perchlorate were purchased from Sigma-Aldrich (Milwaukee, WI). *N, N'*-Dimethylethanolamine, SERALITE SRA-400 anion exchange resin and solvents were purchased from Sisco Research laboratory (Mumbai, India).

Synthesis of O-Acylcholines. OACs with even acyl chainlengths (*n* =12-20) were synthesized in two steps. In the first step the fatty acid was condensed with *N*, *N'*-

dimethylethanolamine using dicyclohexylcarbodiimide (DCC) as the coupling agent and 4-dimethylaminopyridine (DMAP) as the catalyst. Fatty acid (1.15 eq), *N*, *N'*-dimethylethanolamine (1.0 eq) and DMAP (0.5 eq) were taken in a round bottom flask and the mixture was azeotroped thrice with dry benzene. The mixture were dried under high vacuum and dissolved in dry dichloromethane. DCC (1.4 eq) was added to the reaction mixture at 0°C. The reaction mixture was stirred overnight raising the temperature from 0°C to room temperature in an inert atmosphere. The condensation product (fatty acid ester of *N*, *N'*-dimethylethanolamine) was extracted with ethyl acetate and purified by column chromatography. The purified and dried ester in dichloromethane was treated with 1.3 eq of methyl iodide at 0 °C for quaternization. The product obtained (*O*-acylcholine iodide) was washed thrice with dry ether and dried under vacuum. The purified OACs were characterized by IR and ^{1}H-NMR spectroscopy.

Conversion of O-Stearoylcholine Iodide to O-Stearoylcholine Chloride. *O*-Stearoylcholine iodide was converted to the corresponding chloride salt by ion exchange using SERALITE SRA-400 anion exchange resin. In order to get complete exchange of the counterion to chloride, the procedure was carried out twice. The purity of the product was characterized by ^{1}H NMR and IR spectroscopy.

Differential Scanning Calorimetry. DSC studies were performed using a VP-DSC equipment from MicroCal (MicroCal LLC, Northampton, MA, USA). Accurately weighed lipid samples (~1 mg) were dissolved in dry chloroform and the solvent was removed under a stream of dry nitrogen gas. The resulting lipid film was vacuum desiccated for 5-6 hrs in order to remove residual traces of the solvent. The lipid was hydrated thoroughly with Millipore water or with 150 mM concentration of the appropriate salt

(Na_2SO_4/NaCl/NaBr/$NaNO_3$/$NaClO_3$/NaI/$NaClO_4$) before performing the heating scans. In all cases the second heating scan was considered for data analysis. Transition enthalpies were determined by integrating peak areas under the transition curves. Transition entropies were determined from the transition enthalpies assuming a first order transition according to the expression:[36,37]

$$\Delta H_t = T_t.\Delta S_t \quad (1)$$

where T_t is the transition temperature and ΔH_t values are taken at this temperature in order to calculate the corresponding ΔS_t values.

Turbidimetry. Samples for turbidimetric measurements were prepared by dispersing OSC in water, or 150 mM NaCl, or 150 mM NaI and heating to about 65-70 °C in a warm water bath with intermittent vortexing, followed by at least three cycles of freeze thawing, using liquid nitrogen and hot water (ca. 70 °C). After the last incubation in hot water, the sample tube was equilibrated to room temperature and transferred to a spectrometer cuvette. Turbidimetric measurements were performed at various temperatures between 20 and 70 °C using a Cary 100 UV-Visible spectrophotometer equipped with a Peltier thermostat supplied by the manufacturer. Turbidity was measured by recording the absorption spectrum between 350 and 450 nm and turbidity at 400 mm was considered for further analysis.

ESR Spectroscopy. Spin-labeled dispersions of OSC containing probe amounts of 5-SASL were prepared as follows. Measured volumes of OSC stocks (dissolved in chloroform) and the spin-label stock were dispensed into glass sample tubes using a Hamilton syringe to yield 0.5 mol% of the spin label in the lipid and the solvent was evaporated by gently blowing dry nitrogen gas. Final traces of the solvent were removed by

vacuum desiccation for at least three hours. The samples were then hydrated with water or with 150 mM NaCl and kept in the dark at room temperature for 3 hrs. Then the samples were centrifuged, and the pellets were transferred to 1 mm diameter glass capillaries. ESR spectra were recorded on a JEOL JES-FA 200 ESR spectrometer equipped with an air-flow temperature regulation system. Samples in 1 mm ID glass capillaries were placed in a standard quartz ESR tube containing light silicone oil for thermal stability. Temperature was measured with a fine-wire thermocouple positioned near the ESR tube.

Crystallization, X-ray Diffraction and Structure Solution. Thin needle type, colorless crystals of *O*-stearoylcholine iodide were grown at room temperature from a mixture of chloroform, methanol and water. A crystal of 0.28 × 0.16 × 0.04 mm size was used for data collection in the present study. X-ray diffraction measurements were carried out at room temperature (ca. 25 °C) with a Bruker SMART APEX CCD area detector system using a graphite monochromator and Mo-Kα (λ = 0.71073 Å) radiation obtained from a fine-focus sealed tube.

Data reduction was done using Bruker SAINTPLUS program. Structure solution was carried out in the triclinic space group. Absorption correction was applied using SADABS program. The structure was solved successfully by direct methods in the space group *P-1* and refinement was done by full matrix least-squares procedure using the SHELXL-97 program.[38] The refinement converged into a final R_1 = 0.186, wR_2 = 0.466 and goodness of fit = 1.54. The somewhat high R_1 and wR_2 may be due to difficulty in growing good quality single crystals. In this context, it may be noted that in general lipids do not yield good quality single crystals. In addition, the diffraction patterns of lipids are dominated by strong

subcell reflections arising from the regular hydrocarbon chain matrix, which complicate or sometimes hinder the structure solution.[39]

Crystal Parameters of O-Stearoylcholine Iodide. Molecular formula: $C_{23}H_{48}INO_2$. Molecular formula weight: 497.5; Crystals were thin-plate type and colorless. Crystal system, triclinic; Space group, Sg = *P*-1; Ambient temperature, T = 298(2) K; Radiation wavelength (λ) = 0.71073 Å; Minimum resolution = 0.84 Å; Radiation type, Mo-Kα; Radiation source, Fine-focus sealed tube; Radiation monochromator, graphite; Number of reflections collected, 24156; Unique reflections, 9303; Reflection with I > 2σ(I), 5930; Number of parameters, 505.

Unit cell dimensions (with standard deviation in parentheses): a = 7.992(3), b = 9.634(4), c = 35.413(14) Å; α = 86.398(7), β = 84.785(8), γ = 89.961(7)º; Volume of the cell, V = 2709.9(19) Å^3; Number of molecules in the unit cell, Z = 4; Angle of tilt of *O*-acyl chains, θ = 1.7°; $F_{(000)}$ = 1064; Absorption Coefficient, μ =0.175 mm^{-1}; T = 298(2) K.

RESULTS

Differential Scanning Calorimetry of O-Acylcholines. *O*-Acylcholine iodides yielded turbid suspensions upon hydration, which settled down over a period of time. The turbid suspensions become optically clear at higher temperatures, suggesting that the amphiphile undergoes a transition from a phase of high turbidity (possibly lamellar gel phase) to a phase where aggregates are small (such as micelles), which do not scatter visible light. In order to characterize the thermotropic phase transitions, DSC studies were carried out on hydrated *O*-acylcholines (OACs) of even acyl chains (n = 12-20). OACs with different acyl chains

exhibit a single, broad transition, except *O*-arachidoylcholine which showed a minor transition before the main transition. Representative heating thermograms of OACs dispersed in water are shown in Figure 1A. Transition temperatures (T_t), widths at half maximum of the transition ($T_{1/2}$), transition enthalpies (ΔH_t) and transition entropies (ΔS_t) obtained from the heating thermograms are presented in Table 1. It is seen from this table that the thermodynamic parameters such as T_t, ΔH_t and ΔS_t increase with increase in the chainlength. As discussed in more detail below, a linear chainlength dependence was observed for ΔH_t and ΔS_t for the OACs of even chainlengths, indicating that structures of the phases formed by all OACs in aqueous dispersions are likely to be very similar. Therefore, a detailed characterization of the phase structure and phase transitions exhibited by one of the molecules in the series is likely to give a fairly good idea of the phase structures adopted by the entire homologous series. In view of this, further studies regarding the phase structure and phase transition were carried out with *O*-stearoylcholine iodide.

Calorimetric Studies in the Presence of Hofmeister Ions. Further studies with OSC were performed in the presence of 150 mM NaCl (physiological salt concentration), or 150 mM NaI in order to investigate the role of chloride and iodide on the phase behavior. Representative heating thermograms in water, in 150 mM NaCl and in 150 mM NaI are shown in Figure 1B. It was observed that in the presence of 150 mM NaCl the phase transition temperature (T_t) decreases from 61.4 to 37.7 °C, whereas it increases to 64.6 ºC in the presence of 150 mM NaI (Figure 1B). DSC studies were also performed with OSC at different concentrations of NaCl (25 mM to 1M) and the thermodynamic parameters estimated from the thermograms are listed in Table S1.

To investigate the phase behavior of OSC in the presence of other anions, DSC studies were performed with samples containing Na_2SO_4, $NaNO_3$, NaBr, $NaClO_3$ or $NaClO_4$ at 150 mM concentration. It may be noted that while Na_2SO_4 is a kosmotrope, the remaining salts are all chaotropes. Thermograms obtained from these studies are presented in Figure 2 and thermodynamic parameters estimated from them are summarized in Table 2. It is seen from Figure 2 and Table 2 that the transition temperature increases along the Hofmeister series: Na_2SO_4 < NaCl < NaBr < $NaNO_3$ < $NaClO_3$ < NaI < $NaClO_4$.

Turbidimetric Studies on OSC. The thermotropic phase transition of OSC was further characterized by tubidimetric studies, monitoring the turbidity at 400 nm as a function of temperature using a spectrophotometer. Figure 3 depicts the temperature dependence of turbidity of OSC in water, in 150 mM NaCl and in 150 mM NaI. In all three environments the turbidity at low temperature was relatively high and remains constant with increase in temperature initially but exhibits a sharp decrease over a narrow temperature range and thereafter remains at a constant level. The midpoint of the steeply declining region was taken as the phase transition temperature (T_t). The T_t values obtained from the turbidimetric studies were 57.5, 34.3 and 62.0 °C, respectively, for measurements performed in water, in 150 mM NaCl and in 150 mM NaI. These values are slightly lower than the values obtained from the DSC measurements, but are consistent with the DSC results in that the phase transition temperature decreases by over 20 degrees in the presence of 150 mM NaCl and slightly increases in presence of 150 mM NaI. From Figure 3 it can be clearly seen that turbidity of the sample before phase transition in water is much higher as compared to the turbidity of the sample prepared in 150 mM NaCl. Visual inspection also indicated that the sample (0.05 wt%) prepared in water is highly turbid as compared to the sample of the same concentration

prepared in 150 mM NaCl (Figure 4A, B). This suggests that ions can modulate the phase structure, and consequently, phase transition temperature (Krafft temperature) of OSC. Both samples were optically clear above T_t, indicating that the aggregates are relatively small, which most likely correspond to micelles.

In order to investigate the modulation of phase structure by salt, turbidimetric studies were performed with hydrated dispersions of OSC. In these experiments, small aliquots of NaCl from a 2 M stock solution were added to a suspension of OSC in water. Results of such titrations, performed at 30 ^{o}C (below the phase transition temperature of OSC hydrated with water as well as 150 mM NaCl) and at 45 ^{o}C (which is above T_t when hydrated with 150 mM NaCl, but below T_t when hydrated with water alone) are shown in Figure 4C. The data presented in this Figure show that at 45^{o}C increase in NaCl concentration results in a steep decrease in the turbidity of the OSC suspension in a narrow window of NaCl concentration (ca. 0-25 mM) and yields a nearly optically clear solution. The sample remains clear when the NaCl concentration is increased further (up to 200 mM). On the other hand, titrating an OSC suspension with NaCl at 30 ^{o}C (which is below the phase transition temperature of the sample hydrated by water or 150 mM NaCl) did not lead to any sharp changes in the turbidity. Only a steady decrease in the turbidity was observed with increase in the chloride concentration. Since the transition observed at 45^{o}C is induced by the addition of ions, the phenomenon is basically an ion-induced phase transition and we refer to this as *chaotropic phase transition*. As OACs with different chainlengths are isostructural, it is expected that the other OACs will also undergo similar ion-induced phase transitions.

Spin-Label ESR Spectroscopy. Spin-label ESR spectroscopy enables the study of specific environments within lipid aggregates and membranes. The outer hyperfine splitting

($2A_{max}$), which gives a measure of anisotropic motion of the probe, provides information regarding the structure and dynamics of lipid aggregates. The ESR spectra of 5-doxyl stearic acid (5-SASL) incorporated at probe concentration in OSC, dispersed in water and in 150 mM NaCl recorded at different temperatures are shown in Figures 5A & 5B, respectively. At 25 °C the spectra recorded in water and in 150 mM NaCl exhibit strong spin-spin broadening, clearly indicating that in this phase the acyl chains of OSC are tightly packed. The $2A_{max}$ value of 5-SASL in OSC at 25 ^{o}C was found to be 64.1 G and 61.7 G, respectively in water and in 150 mM NaCl. The value of the $2A_{max}$ obtained in water at room temperature is close to the value exhibited by the gel or crystalline phase of lipids and suggests that OSC may adopt a gel or crystalline phase. The $2A_{max}$ value observed in 150 mM NaCl is somewhat smaller and therefore most likely corresponds to the gel phase but not the crystalline phase. The $2A_{max}$ values decrease with increase in temperature with a steep decrease being seen near the phase transition temperature in both the environments. By monitoring the temperature dependence of $2A_{max}$ the phase transition temperature was determined as 58 and 36 °C, respectively, for measurements performed in water and 150 mM NaCl (Figure 5C). These observations are also consistent with a lowering of the phase transition temperature in the presence of 150 mM NaCl, as seen from the results of DSC and turbidimetric studies presented above. In both environments the spectra become more isotropic above the phase transition temperature. Qualitatively similar spectra have been obtained for 5-SASL incorporated in octadecyl-trimethylammonium bromide (C_{18}TAB) micelles[40] and other micelles. This observation, together with the results of the turbidimetric studies presented above, strongly suggests that in water and in 150 mM NaCl OSC exists in a micellar state above the phase transition temperature.

DSC of O-stearoylcholine chloride. Results of DSC measurements with *O*-stearoylcholine chloride (counterion is chloride) dispersed in water are shown in Figure 6. From this figure it can be seen that OSC chloride gives an endothermic transition centered at 18.9 ^{o}C, whereas OSC with iodide counterion gives a transition around 61.4 ^{o}C (see Figure 1 and Table 1). These results demonstrate that counterion plays a definite role in modulating the transition temperature. The transition temperature increases to 32.9 ^{o}C at 150 mM NaCl, which could be due to the screening of the electrostatic repulsion between the charged head groups, resulting in a tightening of the acyl chain packing[41] (Figure 6).

Structure and Packing. Since spectroscopic studies have shown that preferred conformations of acyl chains observed in solid-state by X-ray analyses are predominant also in the gel phase of lipids,[39] determination of the 3-dimentional structure of lipids in the solid state by single crystal X-ray diffraction and analysing the intermolecular interactions will be of immense value in understanding their structure and organization in the hydrated state. Therefore, in the present study, we have determined the 3-dimensional structure of *O*-stearoylcholine iodide (OSC) and analyzed the molecular packing and intermolecular interaction in the crystal lattice. An ORTEP of the molecular structure of *O*-stearoylcholine iodide is shown in Figure S1 and a packing diagram is given in Figure 7. Selected bond distances, bond angles and torsion angles are given in Table S2. The hydrocarbon portion of the acyl chains of OSC adopts an all-*trans* conformation in the solid state, with all the torsion angles in the acyl chain region being close to 180°. The iodide ions are close to the positively charged trimethyl ammonium group with the nitrogen-iodide distance being 4.93 Å. The packing diagram (Figure 7) shows that the OSC molecules are packed in a head-to-tail manner with a common hydrocarbon chain matrix that is confined on both sides by a

boundary layer of polar groups. This type of chain packing, known as interdigitation of acyl chains, accommodates two hydrocarbon chains per head group. In addition to the iodide counter ion, for two OSC molecules, a water molecule is also accommodated in the crystal lattice. The iodide and bulky choline moiety in the polar head group increase the observed molecular area to 38.5 $Å^2$, which is approximately twice that of hydrocarbon chain cross section (19-20 $Å^2$).[42] This is consistent with the formation of the interdigitated bilayer structure. The layer thickness (carbonyl carbon-carbonyl carbon distance) of OSC is 21.8 Å and the all-*trans* acyl chains are nearly perpendicular to the bilayer plane, with a virtually negligible tilt angle of 1.7° with respect to the bilayer normal.

DISCUSSION

Although, as indicated in the introduction, *O*-acylcholines with saturated acyl chains exhibit interesting biological properties and have potential therapeutic applications,[29-35] the phase behavior and structure-activity relationships of OACs are not yet understood. In order gain better understanding about the structure–function relationships for these amphiphiles we have characterized their phase behavior and thermodynamics of phase transitions in aqueous dispersion and investigated the effect of counterions on them. The results obtained are discussed below.

Chainlength Dependence of Transition Enthalpy and Transition Entropy. The chainlength dependence of transition enthalpy and transition entropy for the aqueous phase transitions of OACs of even chainlengths are given in Figures 8A and 8B, respectively. The enthalpy and entropy data for OACs of even chainlengths could be fit well to expressions (2) and (3), given below:[36,43]

$$\Delta H_t = \Delta H_o + (n\text{-}2)\,\Delta H_{inc} \quad (2)$$

$$\Delta S_t = \Delta S_o + (n\text{-}2)\,\Delta S_{inc} \quad (3)$$

where n is the number of C-atoms in the acyl chains and ΔH_o and ΔS_o are the end contributions to ΔH_t and ΔS_t, respectively, arising from the terminal methyl group and the polar region of the OAC molecule. ΔH_{inc} and ΔS_{inc} are the incremental values of ΔH_t and ΔS_t contributed by each CH_2 group. Linear least squares analysis of the chainlength-dependent values of ΔH_t and ΔS_t for the even chainlengths of OACs yielded the incremental values (ΔH_{inc}, ΔS_{inc}) and end contributions (ΔH_o, ΔS_o). These values are listed in Table S3. For the sake of comparison corresponding values obtained with long-chain *N*-acylethanolamines (NAEs) and fatty acids are also given in this Table. The ΔH_{inc} value of 1.82 kcal/mol/CH_2 observed here for the OACs with even chainlengths indicates that the incremental enthalpy contributed by each CH_2 unit in the OACs is higher than that observed with the hydrated NAEs and dry fatty acids.[37] Similarly, the ΔS_{inc} values obtained here for the OACs with even acyl chains are also considerably higher than the ΔS_{inc} values obtained for the NAEs and fatty acids (Table S3). These observations suggest that the acyl chains in OACs are packed more tightly than the acyl chains in NAEs and fatty acids.

Chainlength dependence of transition temperatures. Although the data presented in Table 1 show that the transition temperatures increase with increase in acyl chainlength, the T_t values do not increase in linear proportion to the acyl chainlength. In order to understand this better the transition temperatures have been plotted as a function of acyl chainlength (Figure 8C). From this figure it is seen that the T_t values increase in a smooth progression but with decreasing increments as the chainlength is increased. As the acyl chainlength

increases, the total contribution from the polymethylene portion towards the total enthalpy and entropy of the phase transition will be sufficiently large that the end contributions are negligible in comparison. Therefore, at infinite acyl chainlength, equations (2) and (3) can be reduced to:[36]

$$\Delta H_t = (n\text{-}2)\Delta H_{inc} \quad (4)$$

$$\Delta S_t = (n\text{-}2)\Delta S_{inc} \quad (5)$$

Then the transition temperature for infinite chainlength, T_t^{∞}, will be given by:

$$T_t^{\infty} = \Delta H_{inc}/\Delta S_{inc} \quad (6)$$

From the incremental enthalpy and entropy, the T_t^{∞} value for the OAC of even acyl chainlength has been estimated as 360.4 K. The chainlength dependence of the transition temperatures of OACs of even acyl chainlengths was fitted to eq. 7, predicted from the linear dependence of transition enthalpy and transition entropy given in equations 1 and 2:[44,45]

$$T_t = \Delta H_t/\Delta S_t = (\Delta H_{inc}/\Delta S_{inc})\,[1 - (n_o - n_o')/(n - n_o')] \quad (7)$$

where n_o (= $-\Delta H_o/\Delta H_{inc}$) and n_o' (= $-\Delta S_o/\Delta S_{inc}$) are the chainlengths at which the transition enthalpy and transition entropy, respectively, extrapolate to zero. From the nonlinear least squares fit shown in Figure 8C, it is evident that the transition temperatures of OACs with even chainlengths are described quite accurately by equation 7. In addition, the fitting parameters yielded the transition temperature at infinite chainlength (T_t^{∞}) for the OACs of even acyl chains as 390.7 K with χ^2 of 0.27.

Role of ions on phase behavior. Results obtained from DSC, turbidimetric and ESR spectroscopic studies suggest that the turbid suspensions of OACs, which settled down over a

period of time become optically clear above the transition temperature. As the OACs tend to form precipitates near physiological temperature, their solubility might be very low in this temperature range. Now if their solubility in water is too low and they tend to settle down from the water then the question that rises is, how they are biologically active?

The tendency of surfactants to precipitate from aqueous solutions inhibits their activity and the hydrated solid precipitate can be termed 'inactive state' in view of their lack of activity in this state. As the hydrated solid precipitate transforms to micelles above Krafft temperature, it is desirable to find ways to decrease the Krafft temperature, which would result in an increase in the temperature range over which the surfactant would be active. In the present studies we have found that 150 mM NaCl induces significant changes in the phase properties of OSC and leads to a large decrease in the phase transition temperature (here, Krafft temperature). On the other hand in presence of 150 mM NaI, the phase transition temperature increases slightly as compared to the sample dispersed in water alone (see Figures 1B and 3). In water, in 150 mM NaCl and 150 mM NaI (all the environments) the phase above transition temperature is most likely micellar, as the lipid dispersions were optically clear and have very low optical density as revealed from turbidimetric measurements (Figures 3, 4). The ESR spectra recorded above the phase transition temperature in aqueous dispersions were more isotropic, which also support the micellar structure above the phase transition (Figure 5). Lowering of the transition temperature in the presence of 150 mM NaCl suggest that OACs with chloride counterion exhibit much lower phase transition temperature than when the counterion is iodide. This indicates that ions significantly modulate the phase behavior of OACs. To gain further information regarding the number of ions required in the modulation, OSC with chloride counterion was

synthesized and the DSC studies were performed with an aqueous dispersion of the sample. The results obtained show that OSC with chloride counterion exhibits a much lower phase transition temperature than OSC with iodide counterion (Figure 6). Our result suggest that one ion per lipid molecule in the solution is sufficient to modulate the phase properties of OACs.

The effect of electrostatic interactions on the gel-to-fluid transition of charged phospholipid bilayer membranes have been investigated in detail.[46-48] In such systems, by modulating salt concentration and changing the pH, it was concluded that electrostatic repulsion between the headgroups significanty affects the gel-to-fluid transition,[46-48] although free energy of interaction between the hydrophilic segment and water is also important.[49] While the electrostatic repulsion among charged lipid headgroups favors the fluid phase with disordered acyl chains, the van der Waals attractions favor the chain-ordered gel phase. Thus, the Coulombic interaction competes with van der Waals interaction and below the phase transition temperature the counterions would be expected to be strongly associated with the gel phase thus making the area per headgroup small, whereas above transition temperature counterions would be released into the surrounding aqueous solution (due to entropic reason) leads to the fluid phase. In case of amphiphiles, the release of counterions into aqueous solution makes the lamellar fluid phase very unstable due to electrostatic repulsion and the gel phase transforms directly to micellar phase. We, therefore expect that the electrostatic interactions and counterions could well modulate Krafft transition of ionic surfactants, where the gel(or crystalline) phase-to-micelle transition remains an important parameter for surfactant solubility.

The modulation of Krafft temperature of OSC by ions follows the Hofmeister series, where kosmotropic ions lower the Krafft temperature and chaotropic ions increases the Krafft temperature. The Hofmeister effect for macromolecules (protein, nucleic acids) in aqueous solution are ubiquitous, although precise origin of action of the ions in the series has not yet been understood.[16,18] However, in case of surfactants a fairly good understanding about the role of Hofmeister ions was obtained with the ion-pair formation *vs* hydration arguments[28,50,51]. It was based on law of "matching water affinities" and attributes that chaotropes can form direct ion-pairs with other chaotropes, while kosmotropes would pair only with other kosmotropes, but chaotropes do not come close contact with kosmotropes[28,50,51]. In other words, ions with equal water affinities will associate with each other and tend to form contact ion-pairs in solution, whereas those with differing water affinities will tend to separate.[51] Qualitatively, small cations were found to prefer small anions or anionic groups (e.g., acetate), lead to kosmotrope-kosmotrope interaction, while larger cations (potassium) are attracted to larger anions or anionic groups (e.g., methylsulfate).[28] Since choline group was regarded earlier as a chaotrope[28], it will associate with chaotropic ions and forms contact ion pairs with ions such as iodide, perchlorate, chlorate etc. In such ion pairs, the screening of the charge will be effective and they are likely to be much less hydrated than the individual ion and headgroup. The 3-dimentional structure of OSC iodide ion-pair shows that molecules in the crystal pack in an interdigitated manner that allows both close packing of the alkyl chains (leading to strong van der Waals interactions) and also significant reduction in headgroup repulsion.[52] The moderately chaotropic Cl^-, Br^-, NO_3^- ions are expected to be weakly associated with the choline group and because of the repulsion between the bulky headgroups and hydration they most likely

adopt a tilted bilayer gel phase below Krafft temperature. It would be expected that due to hydration and electrostatic repulsion of the choline headgroups, in the presence of moderately chaotropic and kosmotropic ions the area of headgroup per acyl chain will be more than the ion-pair, formed in the case of strongly chaotropic ions, e.g., iodide.

The insolubilization of the surfactants below Krafft temperature is usually accompanied with the crystallization of alkyl chains (tightly packed bilayer/interdigitated bilayer gel phase) of the surfactant molecules. Above Krafft temperature the system will lose enthalpic stabilization (enthalpy of transition) but will gain more entropy, which leads to the transition from a tightly packed gel to micellar phase. The enthalpy of transition in presence of chaotropic ions is higher than the corresponding enthalpy in presence of weakly chaotropic and kosmotropic ions (Table 2). Mechanistically, the transition from a tightly packed bilayer phase to a micellar phase involves changes in the topology of lipid structures and thus must occur through intermediates involving significant hydrocarbon-water contact. In presence of moderately chaotropic and kosmotropic ions the choline headgroup as well as ions will remain hydrated. This will lead to relatively large headgroup area, which is responsible for loose packing of acyl chains and more water penetration into the bilayer. On the other hand, in the presence of more chaotropic ions the ion-pair formation will lead to screening of charge, resulting in a decrease in the penetration of water into the bilayer. Since the intermediate structure formed during the transition to a micellar phase involves significant water hydrocarbon interaction, the extent of water penetration into the bilayer may also account for the modulation of Krafft temperature. Alternatively, release of counterions into the surrounding aqueous solution above the transition temperature could well explain the observed Hofmeister effect. Strongly associated ions (here chaotropic ions) will be more

reluctant to separate from the ion-pair in the gel or crystalline phase. The removal of counterions from the surface triggers strong electrostatic repulsion and hydration of headgroups, necessary for the formation of micellar phase.

Our present results show that chaotropic ions increase the Krafft temperature of OSC and therefore at physiological temperature these chaotropic ions (such as iodide and perchlorate) induce precipitation and the system behaves as if it is in a virtually inactive state (crystalline phase). On the other hand it exists in an active state (micelle) in presence of chloride counterion at physiological temperature. The Krafft temperature of OSC increases when the ions are changed along the Hofmeister series, suggesting that at a particular temperature the probability of formation of inactive crystalline form increases along the series. This fact will have an important consequence since physiological fluids contain the chloride salts (KCl, NaCl), which may help to keep the lipids and surfactants in their active state at physiological temperature. Similar effect of different ions on proteins has been examined and it was shown that these ions play a definite role in salting-in or salting-out. However, in case of proteins the chaotropic ions induce unfolding and greater solubility, hence salting-in ions and in case of OACs the chaotropes form insoluble ion pairs which lead to precipitation.

SUMMARY AND CONCLUSIONS

Thermotropic phase transitions of a homologous series of *O*-acylcholines, which are biologically relevant lipids, have been characterized by differential scanning calorimetry. A linear dependence has been observed in the thermodynamic parameters, ΔH_t and ΔS_t associated with the chain-melting phase transitions. The first crystal structure in this lipid

series, that of *O*-stearoylcholine iodide has been solved by single crystal X-ray diffraction. The structure demonstrates that the OSC molecules adopt an interdigitated bilayer-type arrangement, with the polymethylene portion of the acyl chains adopting an all-trans conformation. DSC, spectroscopic and turbidimetric studies indicate that in aqueous dispersion *O*-stearoylcholine undergoes a cooperative phase transition from a gel phase to a micellar structure and that the transition temperature increases when the counterions are changed in the Hofmeister series. The OACs in chloride salt environment have a lower Krafft temperature and they will be in active form (micelle) near body temperature, whereas in iodide environment they exist in an inactive state (crystalline precipitate).

Supporting Information Available: Parts of Methods and Results, including three tables (S1 – S3) and two figures (S1, S2) are given in Supporting Information. This material is available free of charge via the internet at http://pubs.acs.org.

ACKNOWLEDGEMENT

This work was supported by a research project from the Department of Science and Technology (India) to MJS. PKT and STR thank the Council of Scientific and Industrial Research (India) for Senior Research Fellowships. We thank the University Grants Commission (India) for their support through the UPE (to University of Hyderabad) and CAS (to School of Chemistry) programs. The authors are grateful to Prof. Samudranil Pal and Dr. Abhik Mukhopadhyay of this School for advice in X-ray data analysis.

REFERENCES

(1) Tsujii, K.; Mino, J. Krafft Point Depression of Some Zwitterionic Surfactants by Inorganic Salts. *J. Phys. Chem*. **1978**, *82*, 1610–1614.

(2) Rodriguez, C. H.; Lowery, L. H.; Scamehorn, J. F.; Harwell, J. H. Kinetics of Precipitation of Surfactants. I. Anionic Surfactants with Calcium and with Cationic Surfactants. *J. Surfact. Deterg.* **2001**, *4*, 1–14.

(3) Shinoda, K. *Colloidal Surfactants*, Academic Press: New York. **1963**; p 7.

(4) Shinoda, K.; Hato, M.; Hayashi, T. The Physicochemical Properties of Aqueous Solutions of Fluorinated Surfactants. *J. Phys. Chem*. **1972**, *76*, 909–914.

(5) Aroti, A.; Leontidis, E.; Maltseva, E.; Brezesinski, G. Effects of Hofmeister Anions on DPPC Langmuir Monolayers at the Air-Water Interface. *J. Phys. Chem. B* **2004**, *108*, 15238–15245.

(6) Leontidis, E.; Aroti, A.; Belloni, L. Liquid Expanded Monolayers of Lipids as Model Systems to Understand the Anionic Hofmeister Series. 1. A tale of models. *J. Phys. Chem. B* **2009**, *113*, 1447–1459.

(7) Klaus, A.; Tiddy, G. J.; Rachel, R.; Trinh, A. P.; Maurer, E.; Touraud, D.; Kunz, W. Hydrotrope-Induced Inversion of Salt Effects on the Cloud Point of an Extended Surfactant. *Langmuir* **2011**, *27*, 4403-4411.

(8) Müller, W.; Déjugnat, C.; Zemb, T.; Dufrêche, J. F.; Diat, O. How do Anions Affect Self-Assembly and Solubility of Cetylpyridinium Surfactants in Water. *J. Phys. Chem. B* **2013**, *117*, 1345-1356.

(9) Manet, S.; Karpichev, Y.; Dedovets, D.; Oda, R. Effect of Hofmeister and Alkylcarboxylate Anionic Counterions on the Krafft Temperature and Melting Temperature of Cationic Gemini Surfactants. *Langmuir* **2013**, *29*, 3518-3526.

(10) Jendrasiak, G. L. Halide Interaction with Phospholipids: Proton Magnetic Resonance Studies. *Chem. Phys. Lipids* **1972**, *9*, 133–146.

(11) Loshchilova, E.; Karvaly, B. Laser Raman Studies of Molecular Interactions with Phosphatidylcholine Multilayers. II. Effects of Mono- and Divalent Ions on Bilayer Structure. *Biochim. Biophys. Acta* **1978**, *514*, 274–285.

(12) Epand, R. M.; Bryszewska, M. Modulation of the Bilayer to Hexagonal Phase Transition and Solvation of Phosphatidylethanolamines in Aqueous Salt Solutions. *Biochemistry* **1988**, *27*, 8776–8779.

(13) Cunningham, B. A.; Lis, L. J. Thiocyanate and Bromide Ions Influence the Bilayer Structural Parameters of Phosphatidylcholines Bilayers. *Biochim. Biophys. Acta* **1986**, *861*, 237–242.

(14) Rydall, J. R.; Macdonald, P. M. Investigation of Anion Binding to Neutral Lipid Membranes Using ^{2}H NMR. *Biochemistry* **1992**, *31*, 1092–1099.

(15) Clarke, R. J.; Lüpfert, C. Influence of Anions and Cations on the Dipole Potential of Phosphatidylcholine Vesicles: A basis for the Hofmeister effect. *Biophys. J.* **1999**, *76*, 2614–2624.

(16) Gurau, M. C.; Lim, S-M.; Castellana, E. T.; Albertorio, F.; Kataoka, S.; Cremer, P. S. On the Mechanism of the Hofmeister Effect. *J. Am. Chem. Soc*. **2004**, *126*, 10522–10523.

(17) Sachs, J. N.; Woolf, T. B. Understanding the Hofmeister Effect in Interactions Between Chaotropic Anions and Lipid Bilayers: Molecular Dynamics Simulations. *J. Am. Chem. Soc*. **2003**, *125*, 8742–8743.

(18) Aroti, A.; Leontidis, E.; Dubois, M.; Zemb, T. Effects of Monovalent Anions of the Hofmeister Series on DPPC Lipid Bilayers. Part I: Swellinmg and in-Plane Equations of State. *Biophys. J*. **2007**, *93*, 1580–1590.

(19) Sanderson, P. W.; Lis, L. J.; Quinn, P. J.; Williams, W. P. The Hofmeister Effect in Relation to Membrane Lipid Phase Stability. *Biochim. Biophys. Acta* **1991**, *1067*, 43–50.

(20) Nguyen, D.; Bertrand, G. L. Calorimetric Observations of the Sphere-Rod Transition of Tetradecyltrimethylammonium Bromide and Sodium Dodecyl Sulfate: Effects of Electrolytes and Non-Electrolytes at 25 and 45 °c. *J. Colloid Int. Sci.* **1992**, *150*, 143–157.

(21) Leontidis, E. Hofmeister Anion Effects on Surfactant Self-Assembly and the Formation of Mesoporous Solids. *Curr. Opin. Colloid Int. Sci*. **2002**, *7*, 81–91.

(22) Anacker, E. W.; Ghose, H. M. Counterions and Micelle Size. I. Light Scattering by Solutions of Dodecyltrimethylammonium Salts. *J. Phys. Chem*. **1963**, *67*, 1713–1716.

(23) Anacker, E. W.; Ghose, H. M. Counterions and Micelle Size. II. Light Scattering by Solutions of Cetylpyridinium Salts. *J. Am. Chem. Soc*. **1968**, *90*, 3161–3166.

(24) Klein, R.; Dutton, H.; Diat, O.; Tiddy, G.J.; Kunz, W. Thermotropic Phase Behavior of Choline Soaps. *J. Phys Chem. B* **2011**, *115*, 3838-3847.

(25) Rengstl, D.; Diat, O.; Klein, R.; Kunz, W. Influence of Chain Length and Double Bond on the Aqueous Behavior of Choline Carboxylate Soaps. *Langmuir* **2013**, *29*, 2506-2519.

(26) Chu, Z.; Feng, Y. Empirical Correlations between Krafft Temperature and Tail Length for Amidosulfobetaine Surfactants in the Presence of Inorganic Salt. *Langmuir* **2012**, *28*, 1175-1181.

(27) Underwood, A. L.; Anacker, E. W. Counterion Lyotropy and Micelle Formation. *J. Colloid Int. Sci.* **1987**, *117*, 242–250.

(28) Vlachy, N.; Jagoda-Cwiklik, B.; Vácha, R.; Touraud, D.; Jungwirth, P.; Kunz, W. Hofmeister Series and Specific Interactions of Charged Headgroups with Aqueous Ions. *Adv. Colloid Interface Sci.* **2009**, *146*, 42-47.

(29) Cho, K. S.; Proulx, P. Lysis of Erythrocytes by Long-Chain Acyl Esters of Carnitine. *Biochim. Biophys. Acta* **1969**, *193*, 30–35.

(30) Cho, K. S.; Proulx, P. Studies on the Mechanism of Hemolysis by Acyl Carnitines, Lysolecithins and Acyl Cholines. *Biochim. Biophys. Acta* **1971**, *225*, 214–223.

(31) Goldberg, A. S.; Wasylyk, J.; Renna, S.; Reisman, H.; Nair, A. S. Isolation and Structural Elucidation of an Ichthyocrinotoxin from the Smooth Trunkfish (*Lactophrys Triqueter* Linnaeus). *Toxicon* **1982**, *20*, 1069–1074.

(32) Jinsart, W.; Ternai, B.; Polya, G. M. Inhibition and Activation of Wheat Embryo Calcium-Dependent Protein Kinase and Inhibition of Avian Myosin Light Chain Kinase by Long Chain Aliphatic Amphiphiles. *Plant Sci*. **1991**, *78*, 165–175.

(33) Schneider, R.; Timms, A. R. Some Aspects of the Pharmacology of an Homologous Series of Choline Esters of Fatty Acids. *Br. J. Pharmacol*. **1957**, *12*, 30–38.

(34) Loftsson, T.; Somogyi, G.; Bodor, N. Effect of Choline Esters and Oleic Acid on the Penetration of Acyclovir, Estradiol, Hydrocortisone, Nitroglycerin, Retinoic Acid and Trifluorothymidine Across Hairless Mouse Skin *In Vitro*. *Acta Pharm. Nordica* **1989**, *1*, 279–86.

(35) Ahlström, B.; Chelminska-Bertilsson, M.; Thompson, R. A.; Edebo, L. Long-Chain Alkanoylcholines, A New Category of Soft Antimicrobial Agents that are Enzymatically Degradable. *Antimicrob. Agents Chemother*. **1995**, *39*, 50–55.

(36) Larsson, K. Physical Properties–Structural and Physical Characteristics. In *The Lipid Handbook*; Gunstone, F. D., Harwood, J. L., Padley, F. B., Eds.; Chapman and Hall: London, **1986**; p 321–384.

(37) Ramakrishnan, M.; Sheeba, V.; Komath, S. S.; Swamy, M. J. Differential Scanning Calorimetric Studies on the Thermotropic Phase Transitions of Dry and Hydrated Forms of *N*-Acylethanolamines of Even Chainlengths. *Biochim. Biophys. Acta* **1997**, *1329*, 302–310.

(38) Sheldrick, G. M. SHELXL97. Program for the Refinement of Crystal Structures. University of Göttingen, Göttingen, Germany, **1997**.

(39) Pascher, I.; Lundmark, M.; Nyholm, P. G.; Sundell, S. Crystal Structures of Membrane Lipids. *Biochim. Biophys. Acta* **1992**, *1113*, 339–373.

(40) Benatti, C. R.; Feitosa, E.; Fernandez, R. M.; Lamy-Freund, M. T. Structural and Thermal Characterization of Dioctadecyldimethylammonium Bromide Dispersions by Spin Labels. *Chem. Phys. Lipids* **2001**, *111*, 93–104.

(41) Trauble, H.; Eibl, H. Electrostatic Effects on Lipid Phase Transitions: Membrane Structure and Ionic Environment. *Proc. Natl. Acad. Sci. USA* **1974**, *71*, 214–219.

(42) Harkins, W. D. *The Physical Chemistry of Surface Films*, Reinhold: New York, **1952**: p 116.

(43) Kamlekar, R. K.; Tarafdar, P. K.; Swamy, M. J. Synthesis, Calorimetric Studies, and Crystal Structures of *N*, *O*-Diacylethanolamines with Matched Chains. *J. Lipid. Res*. **2010**, *51*, 42–52.

(44) Marsh, D. Biomembranes. In *Supramolecular Structure and Function*; Pifat, G., Herak, J. N., Eds.; Plenum Press: New York, **1982**; p 127–178.

(45) Marsh, D. Analysis of the Chainlength Dependence of Lipid Phase Transition Temperatures: Main and Pretransitions of Phosphatidylcholines; Main and Non-Lamellar Transitions of Phosphatidylethanolamines. *Biochim. Biophys. Acta* **1991**, *1062*, 1–6.

(46) Träuble, H.; Teubner, M.; Woolley, P.; Eibl, H. Electrostatic Interactions at Charged Lipid Membranes. 1. Effects of pH and Univalent Cations on Membrane Structure. *Biophys. Chem.* **1976**, *4*, 319-342.

(47) Jähnig, F.; Harlos, K.; Vogel, H.; Eibl, H. Electrostatic Interactions at Charged Lipid Membranes. Electrostatically Induced Tilt. *Biochemistry.* 1979, 18, 1459-1468.

(48) Cevc, G.; Watts, A.; Marsh, D. Titration of the Phase Transition of Phosphatidylserine Bilayer Membranes. Effects of pH, Surface Electrostatics, Ion Binding and Head Group Hydration. *Biochemistry* **1981**, *20*, 4955-4965.

(49) Furuike, S.; Levadny, V.G.; Li, S. J.; Yamazaki, M. Low pH Induces an Interdigitated Gel to Bilayer Gel Phase Transition in Dihexadecylphosphatidylcholine Membrane. *Biophys. J.* **1999**, *77*, 2015-2023.

(50) Collins, K. D. Charge Density-Dependent Strength of Hydration and Biological Structure. *Biophys. J.* **1997**, *72*, 65-76.

(51) Collins, K. D.; Neilson, G. W.; Enderby, J. E. Ions in Water: Characterizing the Forces that Control Chemical Processes and Biological Structure. *Biophys. Chem*. **2007**, *128*, 95-104.

(52) Davey, T. W.; Ducker, W. A.; Hayman, A. R.; Simpson, J. Krafft Temperature Depression in Quaternary Ammonium Bromide Surfactants. *Langmuir* **1998**, *14*, 3210–3213.

Table 1. Transition temperatures (T_t), transition enthalpies (ΔH_t), and transition entropies (ΔS_t) associated with the phase transition of hydrated *O*-acylcholines with even acyl chains. Values of transition enthalpies correspond to averages obtained from a minimum of three independent measurements. All the samples were dispersed in distilled water.

Acyl chainlength (n)	T_t (°C)	$T_{1/2}$	ΔH_t (kcal.mol^{-1})	ΔS_t (cal.mol^{-1}.K^{-1})
12	38.3	2.4	7.1 ± 0.8	22.8
14	48.2	2.6	11.4 ± 1.2	35.5
16	56.2	2.5	15.4 ± 0.8	46.7
18	61.4	2.1	18.3 ± 0.3	54.7
20	67.3	0.9	21.7 ± 1.5	63.7

Table 2. Effect of counterion on the phase transition temperature of OSC. Samples were dispersed in distilled water containing the sodium salt of each anion at 150 mM concentration.

Anion	T_t (°C)	ΔH_t (kcal.mol^{-1})
SO_4^{2-}	33.9	4.1
Cl^-	37.7	8.4
Br^-	40.5	4.9
NO_3^-	41.4	4.0
ClO_3^-	52.4	11.3
I^-	64.6	21.4
ClO_4^-	75.7	11.5

Figure Legends

Figure 1. DSC heating thermograms of *O*-acylcholines. A) Thermograms of OACs with even number of C-atoms in the acyl chains. B) Thermograms of *O*-stearoylcholine dispersed in water, 150 mM NaCl and 150 mM NaI.

Figure 2. Effect of Hofmeister anions on the gel-fluid phase transition of aqueous dispersions of *O*-stearoylcholine. Sodium salts of different counterions were used at 150 mM concentration. The counterions are indicated against the thermograms.

Figure 3. Turbidimetric measurements on the thermotropic phase transition of OSC dispersed in water (●), in 150 mM NaCl (○) and in 150 mM NaI (□). Lipid concentration was 1 mg/ml for all samples.

Figure 4. Snapshot of OSC dispersed in (**A**) water and (**B**) 150 mM NaCl. **C)** Effect of NaCl on the turbidity of OSC at (●) 30 ^{o}C and (○) 45 ^{o}C.

Figure 5. ESR spectra of 5-SASL in OSC dispersed in (**A**) water and (**B**) 150 mM NaCl. In each panel, the spectra were normalized to the same central peak height. **C**) Temperature dependence of $2A_{max}$ (G) in water (●) and in 150 mM NaCl (○).

Figure 6. DSC heating thermograms of *O*-stearoylcholine chloride dispersed in water and 150 mM NaCl.

Figure 7. A packing diagrams of OSC. Acyl chains of OSC pack in an interdigitated manner. The iodide counterions and hydrated water molecules are also shown the packing.

Color code: grey, carbon; red, oxygen; blue, nitrogen; violet, iodine; green, water molecule; white, hydrogen.

Figure 8. Chainlength dependence of thermodynamic parameters of OACs obtained from DSC studies. Transition enthalpies (**A**) and transition entropies (**B**) obtained for the thermotropic phase transitions of *O*-acylcholines of even chainlengths are plotted against the number of methylene units (*n*-2, where n is the number of C-atoms) in each acyl chain. (C) Chainlength dependence of phase transition temperatures of *O*-acylcholines even acyl chainlengths. Solid lines in A and B represent linear least squares fits of the data, whereas in C the solid line corresponds to non-linear least squares fits of the transition temperatures to equation 7.

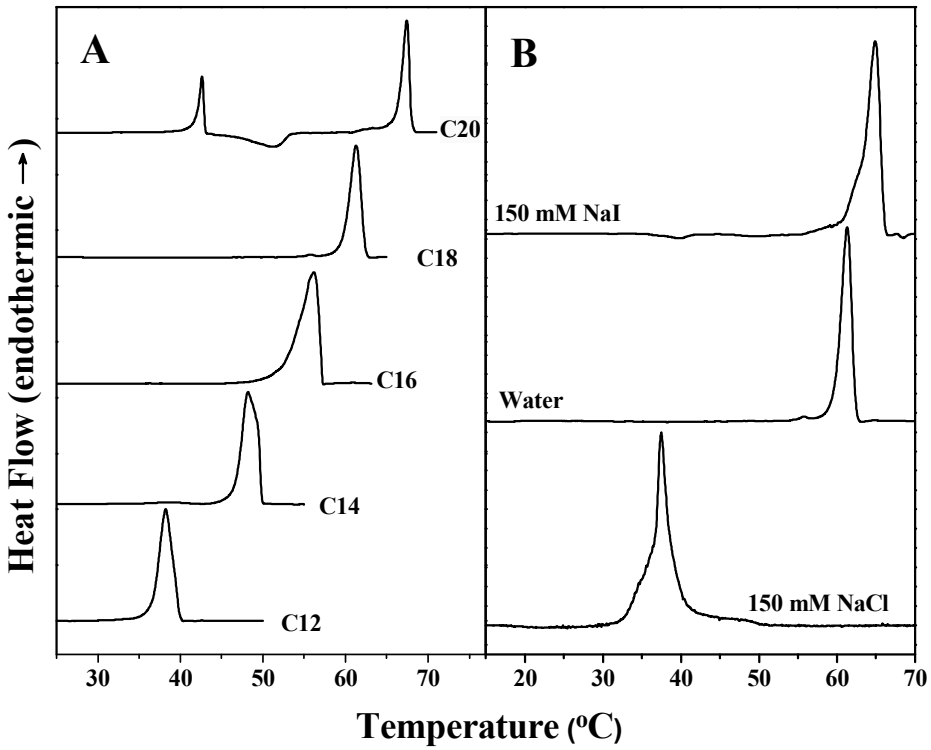
A
B
C20
C18
C16
C14
C12
150 mM NaI
Water
150 mM NaCl
Heat Flow (endothermic →)
30
40
50
60
70
20
30
40
50
60
70
Temperature (°C)

Figure 1

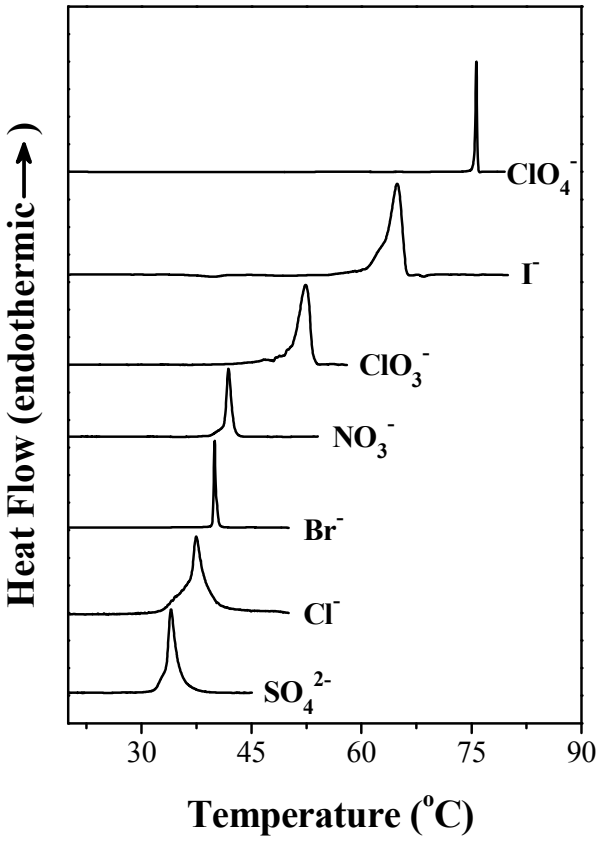
Heat Flow (endothermic⟶)
ClO4-
I-
ClO3-
NO3-
Br-
Cl-
SO4 2-
30
45
60
75
90
Temperature (°C)

Figure 2

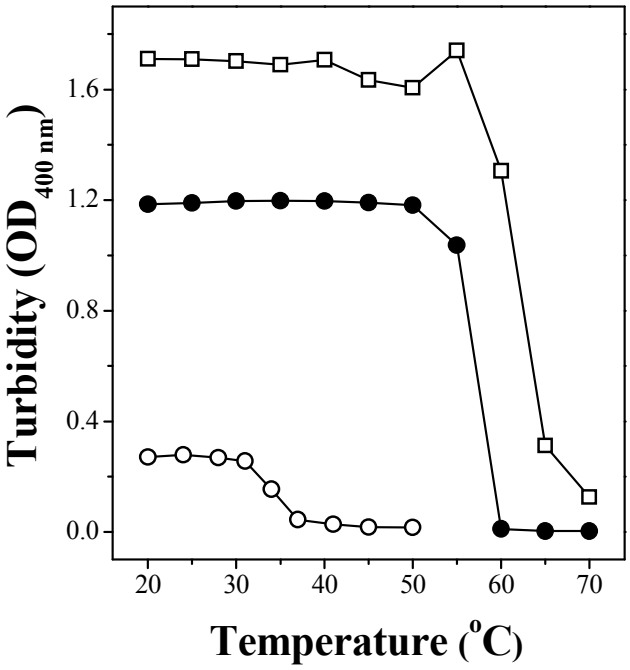
Turbidity ($OD_{400\ nm}$)
1.6
1.2
0.8
0.4
0.0
20
30
40
50
60
70
Temperature (^{o}C)

Figure 3

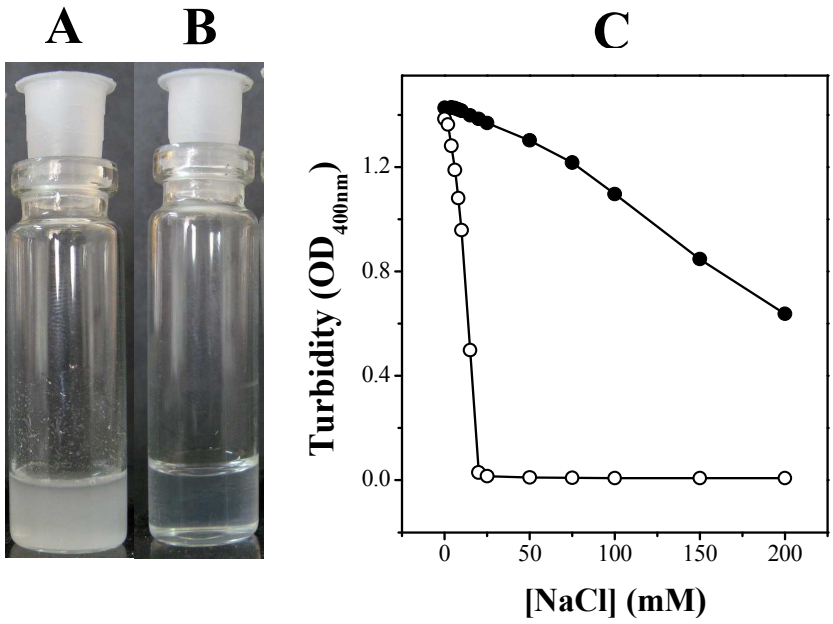

Figure 4

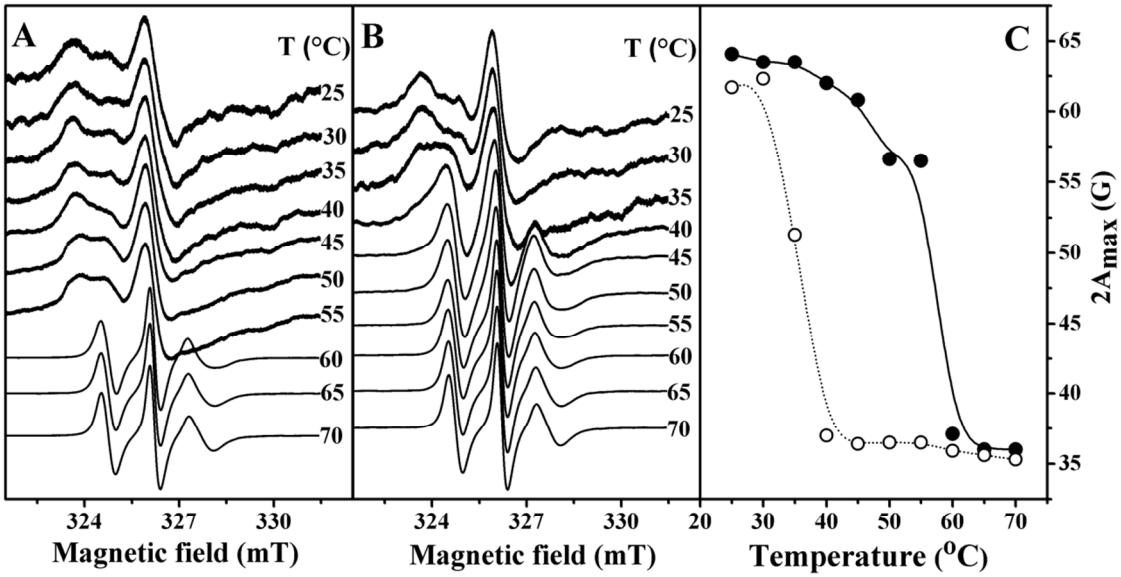
A
T (°C)
25
30
35
40
45
50
55
60
65
70
324
327
330
Magnetic field (mT)
B
T (°C)
25
30
35
40
45
50
55
60
65
70
324
327
330
Magnetic field (mT)
C
65
60
55
50
45
40
35
2Amax (G)
20
30
40
50
60
70
Temperature (°C)

Figure 5

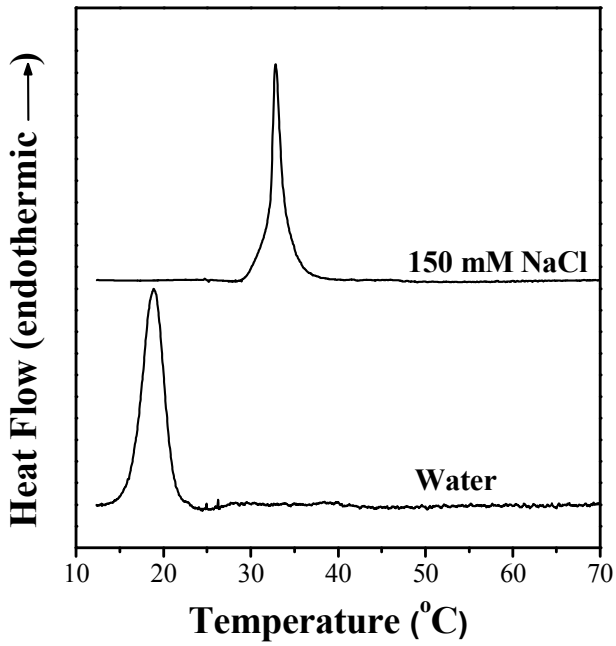
Heat Flow (endothermic ⟶)
150 mM NaCl
Water
10
20
30
40
50
60
70
Temperature (°C)

Figure 6

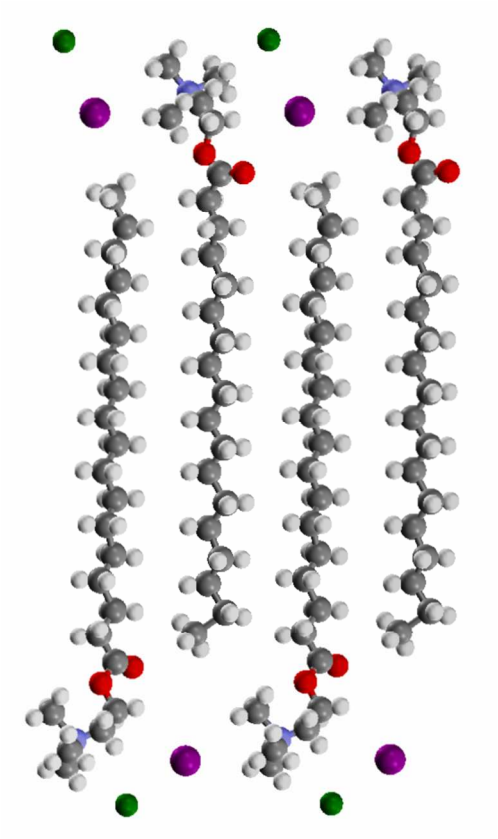

Figure 7

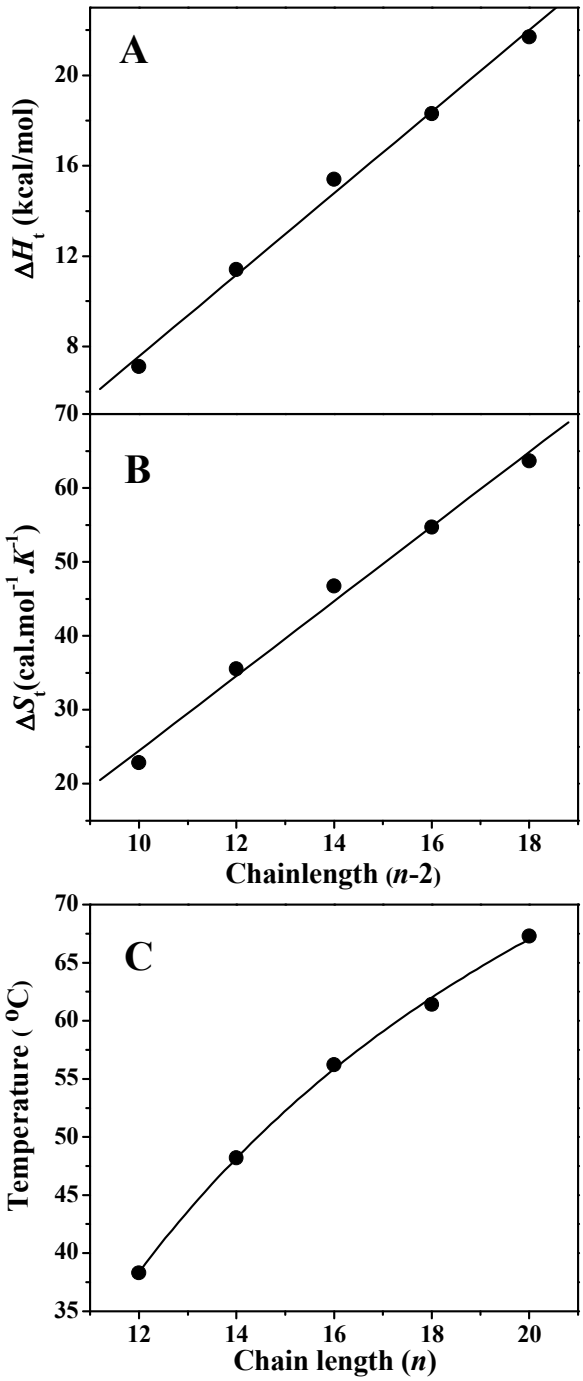
A
ΔH_t (kcal/mol)
20
16
12
8
B
ΔS_t(cal.mol^{-1}.K^{-1})
70
60
50
40
30
20
10
12
14
16
18
Chainlength (*n*-2)
C
Temperature (^{o}C)
70
65
60
55
50
45
40
35
12
14
16
18
20
Chain length (*n*)

Figure 8

For Table of Contents Only

EFFECT OF HOFMEISTER SERIES ANIONS ON THE THERMOTROPIC PHASE BEHAVIOR OF BIOACTIVE *O*-ACYLCHOLINES

Pradip K. Tarafdar, S. Thirupathi Reddy and Musti J. Swamy*

School of Chemistry, University of Hyderabad, Hyderabad - 500 046, India